JCTC Journal of Chemical Theory and Computation

Article

pubs.acs.org/JCTC

Path Integral Metadynamics

Ruge Quhe,[†,‡] Marco Nava,*[,†] Pratyush Tiwary,[†] and Michele Parrinello*[,†]

[†]Department of Chemistry and Applied Biosciences, ETH Zurich, and Facoltà di Informatica, Istituto di Scienze Computazionali, Università della Svizzera Italiana, Via G. Buffi 13, 6900 Lugano, Switzerland

[‡]State Key Laboratory of Mesoscopic Physics, Department of Physics and Academy for Advanced Interdisciplinary Studies, Peking University, Beijing 100871, P. R. China

Supporting Information

ABSTRACT: We develop a new efficient approach for the simulation of static properties of quantum systems using path integral molecular dynamics in combination with metadynamics. We use the isomorphism between a quantum system and a classical one in which a quantum particle is mapped into a ring polymer. A history dependent biasing potential is built as a function of the elastic energy of the isomorphic polymer. This enhances fluctuations in the shape and size of the necklace in a controllable manner and allows escaping deep energy minima in a limited computer time. In this way, we are able to sample high free energy regions and cross barriers, which would otherwise be insurmountable with unbiased methods. This substantially improves the ability of finding the global free energy minimum as well as exploring other metastable states. The performance of the new technique is demonstrated by illustrative applications on model potentials of varying complexity.

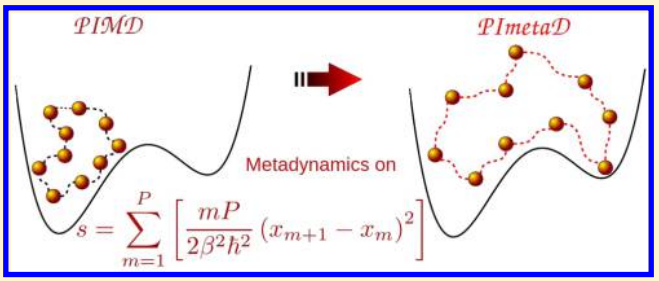

INTRODUCTION

A practical way of simulating quantum systems is to use Feynman's path-integral representation of quantum statistical physics.[1] Neglecting quantum exchanges, this amounts to mapping a quantum system into a classical one in which each particle is replaced by a ring polymer composed of P beads interacting through harmonic springs. The isomorphism becomes more and more exact as $P \to \infty$. A vast number of applications of this isomorphism can be found in literature.[2−4] In this paper, we address the problem of improving the sampling of the classical isomorphism with special emphasis on its inability of overcoming large barriers. This is a universal and much studied problem that plagues all sampling methods. In a quantum system, the ability to cross barriers is enhanced by tunneling, and this feature has been exploited in nonlinear optimization methods[5−8] and very recently for enhancing the sampling of classical Hamiltonians.[9] However, as we shall show below, often this added capability is not enough to cross large barriers in a finite computation time. This difficulty is exacerbated if one uses a small value of P.

The reason for this difficulty can be understood if one observes that in the classical isomorphism the polymer moves from one well to another by stretching over the barrier.[10] The elastic energy associated with these stretched configurations is high, hence during an unbiased simulation they are very rarely, if ever, visited. During the past few years, several methods[11−13] have been suggested to enhance the probability of observing rare events in classical statistical mechanics. In particular, our group has developed metadynamics, a powerful sampling method that has been applied to a large number of systems described by a classical Hamiltonian.[14−16] In this paper, we apply metadynamics to a quantum system described by the quantum−classical isomorphism and demonstrate its ability to enhance quantum tunneling.

A crucial step in any metadynamics calculation is the identification of appropriate collective variables (CVs) whose fluctuations, when enhanced by metadynamics, make it possible to observe rare barrier crossing events in a finite computational time. To this effect, we could have adapted some of the many CVs that have been introduced in the literature[17] and introduced a bias in a standard fashion. However, the previous discussion on how tunneling takes place in the classical isomorphism suggests a different approach, more directly based on the quantum nature of the system. A natural parameter that discriminates between stretched and crumpled polymers is, in fact, the elastic spring energy of the polymers used to represent the quantum system. This choice as biasing CV can be expected to increase the fluctuations in the spread of the polymers, thus increasing also the likelihood of a tunneling event. Moreover, such a CV is system independent and does not require previous knowledge of the potential energy surface (PES).

This work is organized as follows: In the next section, we give a brief introduction of the methodologies used, in the third section, we present our results for various systems and in the final section our comments and conclusions. In the Supporting Information (SI) we have provided further technical and mathematical details of the methodologies and the simulations.

Received: November 10, 2014
Published: February 6, 2015

DOI: 10.1021/ct501002a
J. Chem. Theory Comput. 2015, 11, 1383−1388

METHOD

Let us consider a single particle in an external potential $U(x)$, described by the Hamiltonian $\hat{H} = -(\hbar^2/2m)\hat{\nabla}^2 + U(\hat{x})$. The extension to the many-body three-dimensional case is straightforward if exchange effects are neglected.

The partition function in the canonical ensemble is expressed through the Feynman path integral as

$$\mathcal{Z} = \lim_{P\to\infty} \left(\frac{mP}{2\pi\beta\hbar^2}\right)^{P/2} \int \mathrm{d}x_1 \cdots \mathrm{d}x_P \; \mathrm{e}^{-\beta U_{\mathrm{eff}}(x_1,\cdots,x_P)} \tag{1}$$

$$U_{\mathrm{eff}}(x_1, \cdots, x_P) = \sum_{i=1}^{P} \left[\frac{mP}{2\beta^2\hbar^2}(x_{i+1} - x_i)^2 + \frac{U(x_i)}{P} \right] \tag{2}$$

where $x_{P+1} = x_1$, m is the particle mass, and $\beta = 1/(k_B T)$ the inverse temperature. For a finite P, the partition function is isomorphic to the configurational integral of a ring polymer composed of P harmonically interacting, classical beads under the action of the external potential $(U(x))/P$. The stiffness of the harmonic interaction, $(mP)/(\beta^2\hbar^2)$, tends to infinity in the classical limit and the radius of the polymer shrinks to zero. On the other hand, in the deep quantum regime, the stiffness of the harmonic interaction is a finite quantity that depends on P; different configurations of the beads are then energetically allowed and the polymer shows fluctuations in its shape. Following the quantum−classical isomorphism, the sampling of $\mathcal{Z}$ can be obtained from the classical molecular dynamics (MD) simulation of a polymer in an external field, coupled to a thermal bath. This approach—known in literature as Path Integral Molecular Dynamics (PIMD)—however, has well-known problems of ergodicity[18] because the topology of the polymer is that of a closed chain of harmonic oscillators; this chain has normal modes of different frequencies and thus the MD simulation should be thermalized so that the energy transfer between these modes is ensured. This has been done, as in ref 19, with a thermostat based on a generalized Langevin equation.

In order to avoid confusion, we want to stress that we use these simulations only for sampling, and to this effect, in the spirit of the work of Parrinello and Rahman,[20,21] we assign artificial masses and an artificial dynamics to the beads. In no way, this dynamics is meant to approximate quantum dynamics as proposed more recently by Manolopoulos.[22]

As discussed in the introduction, we enhance sampling by using metadynamics with $s = \sum_{i=1}^{P}[(mP/(2\beta^2\hbar^2))(x_{i+1}-x_i)^2]$ as CV. With this variable, we construct a time dependent bias potential

$$V(s, t) = \sum_{t'<t} W(t')\exp\left(-\frac{(s - s(t'))^2}{2\sigma_G^2}\right) \tag{3}$$

by depositing at time intervals spaced by τ_G Gaussians of width σ_G. The height of the Gaussian $W(t)$ is determined by the well-tempered equation:[23]

$$W(t) = W(0)\exp\left(-\frac{V(s, t)}{k_B\Delta T}\right) \tag{4}$$

where $W(0)$ is the initial Gaussian height, and ΔT a temperature. It has been shown rigorously that this procedure converges modulo a time dependent constant to[24]

$$F(s) = -\left(1 - \frac{1}{\gamma}\right)V(s, t) \tag{5}$$

where $\gamma = (T + \Delta T)/T$ is the boosting factor, and $F(s)$ is the free energy related to the Boltzmann probability distribution of s by $F(s) = -k_B T \ln P(s)$. An interesting interpretation of eq 5 and of the boosting factor γ is obtained if one expresses it in terms of the probability distribution as

$$P_{WT}(s) \propto P(s)^{1/\gamma} \tag{6}$$

where $P_{WT}(s)$ is the probability distribution of variable s in the biased ensemble. Equation 6 underlines the fact that the well-tempered ensemble[23,25] with spring energy as CV is capable of broadening the spring energy distribution, making it easier for the system to explore the low-probability fluctuations that trigger rare events. Furthermore, the amplitude of these all-important fluctuations can be controlled by γ. Recently,[26] it has been shown how the time dependent constant implicit in eq 5 can be calculated and the following time independent estimator for the free energy has been given:

$$\beta F(s) = -\frac{\gamma V(s, t)}{k_B\Delta T} + \log \int \mathrm{d}s \exp\left(\frac{\gamma V(s, t)}{k_B\Delta T}\right) \tag{7}$$

In the same paper, a reweighting method has also been developed that allows to remove on the fly the effect of the bias and thus calculate with ease the expectation value of any operator. These two new developments have been systematically adopted here.

We dub the use of the spring energy s as CV in metadynamics to sample the partition function in eq 1 as "Path Integral Metadynamics" (PImetaD). Along with the spring energy, if need be one can always use additional CVs or replica exchange schemes to further complement the sampling process, as has been done in traditional metadynamics.[15]

RESULTS AND DISCUSSION

Contrary to other CVs, s does not have a transparent physical meaning except for the fact that its expectation value is connected to the quantum kinetic energy K by the relation:

$$K = \frac{P}{2\beta} - \langle s \rangle \tag{8}$$

An increase in the elastic energy fluctuations would allow the particle to explore wider regions, and thus, from this relation, one would expect that metadynamics influences the delocalization of the particle. However, how this can affect sampling is not obvious and has thus been tested heuristically on systems of increasing complexity.

One Dimensional Harmonic Oscillator. We begin our analysis with an exploratory simulation of the harmonic oscillator. The harmonic oscillator is a commonly used reference system where comparison with analytical exact results is possible. Here we calculated the analytical expression for $F(s)$ as a function of P. The intricacies of this analytical derivation are given in the SI.

Unless otherwise specified, we put $T = 0.1$, $k_B = 1$, $\hbar = 1$ and use a unitary mass. We also set the metadynamics parameters as follows: the bias deposition time interval is $\tau_G = 2 \times 10^3\ \Delta t$, the initial Gaussian height $W(0) = 2\ k_B T$, and the Gaussian width $\sigma_G = 1\ k_B T$. Because s is an extensive property, the energy bias required to enhance fluctuations as well becomes greater with

DOI: 10.1021/ct501002a
J. Chem. Theory Comput. 2015, 11, 1383−1388

the number of degrees of freedom. For this reason, γ needs to be increased with P. No attempt has been made to tune these parameters for efficiency, because at this stage our aim is only to provide a demonstration of principle.

The effectiveness of PImetaD as an enhanced sampling tool is visible in Figure 1, where it is seen that PImetaD explores a far larger range of s than PIMD. The agreement with the analytical result, moreover, is very good for any P.

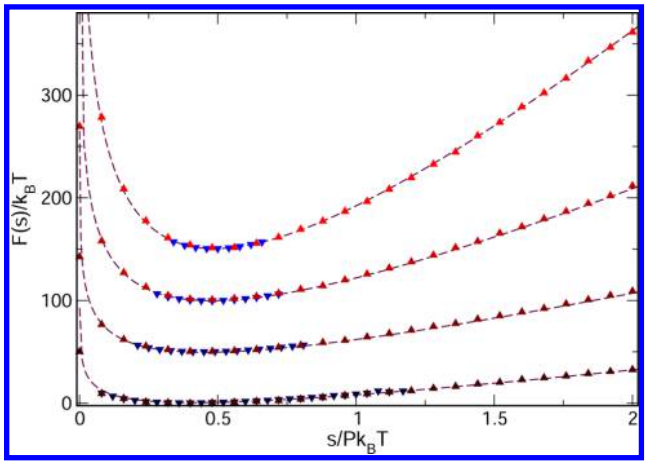

Figure 1. Free energy of the one-dimensional harmonic oscillator as a function of the rescaled spring energy at different values of P (from bottom to up, P = 32, 64, 128, and 256). Dashed lines are the corresponding analytical results. Down triangles denotes data obtained from PIMD, up triangles from PImetaD. The integration time steps, in arbitrary units, are 0.1 (P = 32), 0.07 (P = 64), 0.06 (P = 128), 0.05 (P = 256), and the simulations consist of 10^5 steps. The boosting parameters were adapted to the different P, as follows: γ = 0.5 (P = 32), γ = 1 (P = 64), γ = 2 (P = 128), γ = 4 (P = 256) . For the sake of clarity, we have shifted the different free energies by varying amounts of 40 (P = 64), 80 (P = 128), and 120 (P = 256) in units of k_BT, respectively.

One Dimensional Double Well. We now move to a slightly more complex case where the limits of traditional PIMD can be clearly seen. We study a one-dimensional symmetric double-well potential given by

$$U(x) = -\frac{1}{2}x^2 + bx^4 \tag{9}$$

Here, by varying b, we can regulate the height and the width of the barrier. The curvature of the potential around either of the two minima is 2 in our units. The zero point energy of a unitary mass particle confined to either of the two minima is $E_0 = 1/\sqrt{2}$, which is much higher than the thermal energy at the chosen temperature of 0.1. The probability density is dominated by the symmetric ground state and the first tunnel-split excited state, and thus, we are deeply into the quantum regime.

In order to compare the ability to sample quantum tunneling events of PIMD and PImetaD, we show in Figure 2 $\rho(x)$ for a double-well system with a barrier of 40 k_BT (b = 1/64). The height of the barrier is so high that thermal hopping is not possible, even after the inclusion of zero point effects. Thus, quantum tunneling is mostly responsible for barrier crossing. In Figure 2, we see that PIMD is not able to reproduce tunneling and the system remains trapped in the initial well. Increasing P does not help. Instead, the power of PImetaD is evident since

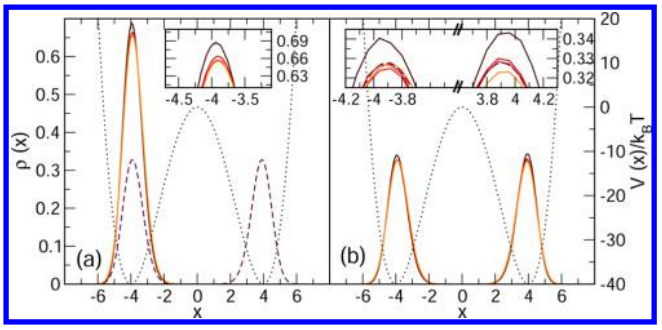

Figure 2. Position probability density in a double-well potential with barrier of $40k_BT$ for (a) PIMD and (b) PImetaD. The value of P is 16, 32, 64, and 128 from dark red to light red. The dashed line is the result obtained from a numerical integration of the Schrödinger equation. The dotted line stands for the external potential. The insets show the details of the probability densities around their maxima. The simulations were 10^7 Δt long, where Δt is 0.09 (P = 16), 0.08 (P = 32), 0.07 (P = 64), and 0.06 (P = 128) in our units.

$\rho(x)$ converges to the numerical solution of the Schrödinger equation.

We can quantify the inefficiency of PIMD if we compare the sampling speed of PIMD and PImetaD. We measure this by computing the characteristic relaxation time τ of the correlation function

$$c_s(t) = \frac{1}{P}\sum_{i=1}^{P}\frac{\langle \xi_i(0)\xi_i(t)\rangle}{\langle \xi_i(0)\xi_i(0)\rangle} \tag{10}$$

where the quantity ξ_i (t) is + or − depending on whether the bead is in the right or in the left well at time t.

If we lower the barrier to 10 k_BT, both PIMD and PImetaD are able to cross the barrier a number of times sufficient to measure τ. It is shown in Figure 3 that PImetaD is substantially

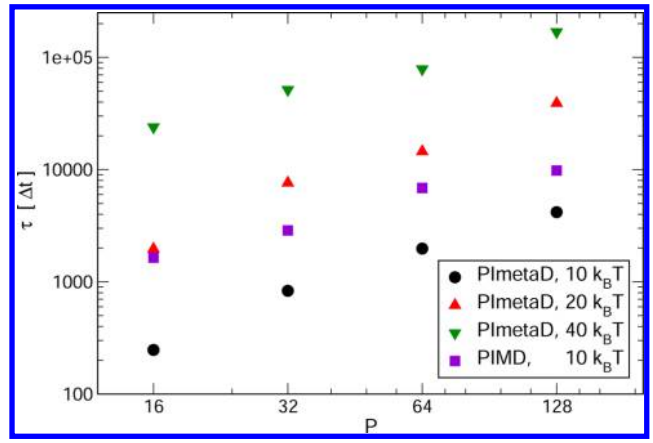

Figure 3. Relaxation time τ as a function of the number of beads P.

more efficient. For larger values of the barrier, we were not able to measure τ in the PIMD case due to insufficient (20 k_BT) or null (40 k_BT) statistics.

We can get more insight into the physics of the tunneling process if we study the fluctuations of the polymer. These fluctuations, in fact, are indirectly connected with the magnitude of the quantum effects. One way to study these fluctuations is through the probability distribution $\rho_c(L,x_c)$, where L is the largest bead−bead distance along the polymer and x_c the polymer center of mass (Figure 4). In the PIMD case

DOI: 10.1021/ct501002a
J. Chem. Theory Comput. 2015, 11, 1383−1388

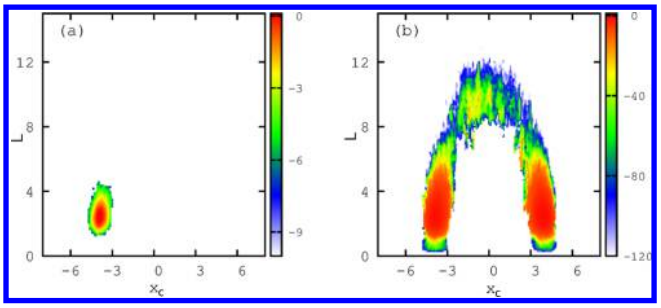

Figure 4. Logarithm of $\rho_c(L,x_c)$ as a function of the longest distance L between beads and the position of centroid x_c in the one-dimensional double-well case from (a) PIMD and (b) PImetaD simulations. The barrier height is 40 k_BT. The number of beads P = 128. Please note the difference in scale between panel a and b.

(left panel), this distribution is very similar to what one would have obtained in the case of a harmonic oscillator. Consistent with Figure 2, the center of mass of the polymer is always in the region around the starting minimum and also the fluctuations of the beads are confined within the well. PImetaD, instead, is able to sample those low probability fluctuations that lead to tunneling. The connection between polymer length fluctuation and tunneling is very evident if we observe that when the polymer is in the classically forbidden region it is maximally stretched.

One Dimensional Multiwell. A natural step forward in complexity from the double-well is the multiwell potential. Following ref 9, we construct a periodic potential by superimposing different plane waves (see SI for details):

$$V(x) = \begin{cases} \sum_{i=1}^{10} a_i \cos\left(\frac{2\pi i x}{L}\right) + b_i \sin\left(\frac{2\pi i x}{L}\right) & -\frac{L}{2} \le x \le 0 \\ V(L-x) & 0 < x \le \frac{L}{2} \end{cases} \quad (11)$$

With the chosen set of parameters $\{a_i, b_i\}$, $V(x)$ has many competing minima separated by high barriers.

As shown in Figure 5 (top panel), near x = 0, there are two, degenerate, local minima A and A′ separated by a barrier h_A = 25 k_BT. The largest barriers in this potential, h_B and $h_{B'}$, have heights ∼70 k_BT, surrounded by the two global minima B and B′ at $x \sim \pm 3$. The calculated position probability densities are plotted in the lower panel of Figure 5, where we also examine the effect of P. As in the double-well case, PIMD (not shown) is not able to explore satisfactorily the entire PES in a reasonable amount of time. Instead, the PES is fully explored by PImetaD.

It is instructive to compare the P = 128 and P = 16 PImetaD cases. The former approaches the exact quantum mechanical solution obtained by numerically solving the Schrodinger equation. It can be seen that, due to quantum effects, the underlying PES features are washed out in the position probability density. Instead, in the P = 16 case the maxima in the density reflect closely the position of the underlying PES. Note, however, that the maximum density is not in correspondence with the positions of the B and B′ absolute minima. This is due to the typical quantum effect that, in this minimum, the curvature is higher, and therefore, due to a larger zero point motion effect, the energy level is pushed up. This observation might be of importance if, as in ref 9, one wants to use the quantum effects to enhance the sampling of classical statistical ensembles. Thus, in the light of suggestions made to use quantum effects to sample complex PES, it would seem that

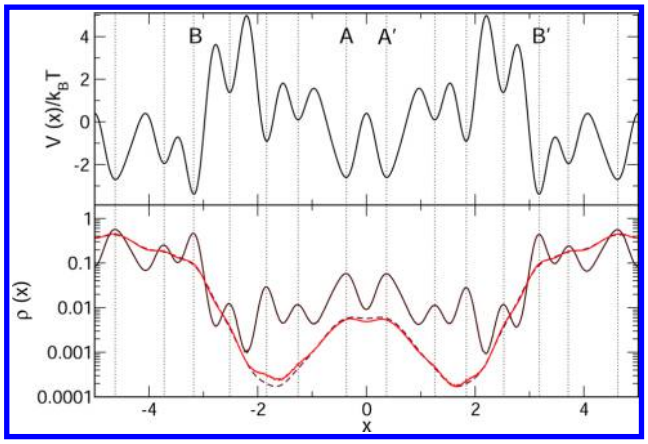

Figure 5. (Top) Multiwell potential and (Bottom) position probability distribution. The dark red and light red curves are PImetaD (P = 16) and PImetaD (P = 128) results. The dashed curve was obtained from the numerical integration of the Schrödinger equation with periodic boundary conditions. The boosting factors γ in the PImetaD simulations are 4 (P = 16) and 12 (P = 128), respectively. The simulations were 10^6 Δt long, where Δt is 0.05 (P = 16) and 0.03 (P = 128) in our units.

using a small P in conjunction with metadynamics might be a better strategy than simply increasing the quantumness of the system.[9,27,28]

PD-H System. As a final example, we now apply PImetaD to a more realistic model representing the behavior of hydrogen in palladium. It is now known that in this system hydrogen diffuses through hoppings between interstitial sites. Earlier classical simulations, using the same model, showed that upon decreasing the temperature the hopping rate quickly exceeds the MD time scale. On the other hand, this is the regime in which quantum effects become relevant.[29,30]

The metal−hydrogen system is thus a useful benchmark for PImetaD. We have applied the methodology to a model composed of one atom of hydrogen inside a bulk palladium FCC crystal consisting of 108 atoms at a density ρ = 0.0593 Å^{-3} using periodic boundary conditions. Only the spring energy of the hydrogen has been biased. The potential model used is the same as that in ref 31, where calculations were performed using classical molecular dynamics for temperatures between 500 and 1000 K. In this regime, the calculations of ref 31 show that the hydrogen sits mainly in the octahedral sites and can move from octahedral site to octahedral site via two mechanisms: either passing first through a tetrahedral site or, less likely, via a straight path that crosses the midway position between two palladiums. We show these channels in Figure 6, where we report the density plot of the hydrogen centroid position within the FCC cell at 400 and 500 K. It is not our purpose here to study the physics of the palladium−hydrogen system, we note, however, again that with PIMD we could not observe one single hopping event in a reasonable amount of computer time even for the largest studied temperature T = 500 K; with PImetaD, instead, a satisfactory sampling was obtained without any input on the possible pathways.

■ CONCLUSIONS

In conclusion, we have developed a new method to enhance sampling of quantum systems by combining PIMD with metadynamics (PImetaD). This new method is demonstrated by applying it to systems of varying complexity and in all the

DOI: 10.1021/ct501002a
J. Chem. Theory Comput. 2015, 11, 1383−1388

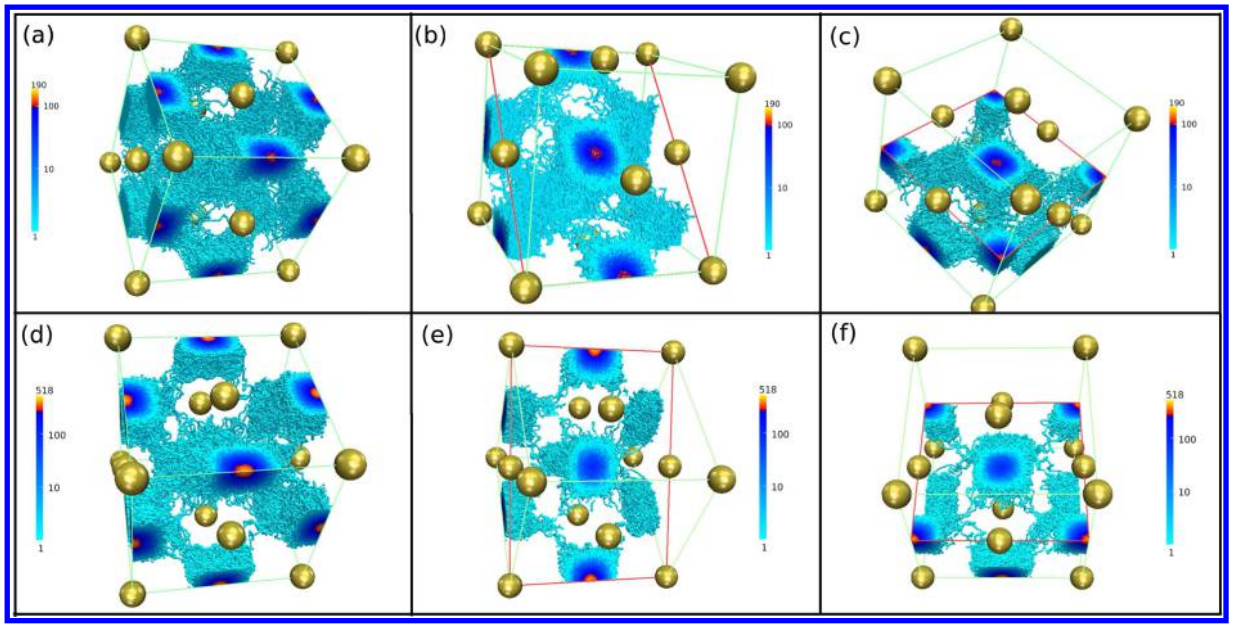

Figure 6. Density plot (in arbitrary units) of the probability distribution of hydrogen in the palladium FCC cell at 500 (upper row) and 400 K (lower row) obtained from the sampled positions of the centroid using PImetaD. Panels b and e are cuts along the surface (1,0,1) and panels c and f are along the (0,0,1/2) surface. Deviations from the cubic symmetry of the distribution are statistical fluctuations of the simulation.

studied cases was found to deal efficiently and easily with the well-known statistical noise and dimensionality issues of the reweighting procedure.[32] In the harmonic oscillator system, we show how PImetaD can sample a larger range of $F(s)$ with respect to PIMD. In the double-well system, we show that PImetaD outperforms PIMD in sampling. This advantage is particularly clear when the barriers between minima are high and wide such that tunneling is rather infrequent. We remark here that even for a 1D double-well, the sampling problem can be nontrivial for PI based methods; this is shown in ref 33 with Path Integral Monte Carlo where, in order to obtain a satisfactory sampling, the introduction of a fictitous quantum kinetic energy was needed. Next, we studied a single particle in one and two-dimensional potentials with multiple energy minima. While the standard PIMD shows poor sampling, PImetaD can efficiently help the particle getting out of the local minima and find the global as well as other local energy minima. In the more realistic case of H in Pd also, we found good results and could explore different reaction pathways without having to specify before neither reaction coordinates nor transition states. Recently, there have been different proposals to improve exploration of complex PES and sampling of classical systems by artificially introducing quantum effects to enhance sampling.[9,27,28] Many of these methods use PIMD as mean to sample tunneling events, and we believe that PImetaD has the potential to enhance further the power of these methods because it enhances the sampling of tunneling effects and can thus supplement the aforementioned methodologies with a more efficient quantum sampling device.

■ ASSOCIATED CONTENT

Supporting Information

Analytical results on the harmonic oscillator; position distribution in the 10 and 20 K_BT double-well case; self correlation functions in the one dimensional double-well case; parameters of the one dimensional multiwell. This material is available free of charge via the Internet at http://pubs.acs.org.

■ AUTHOR INFORMATION

Corresponding Authors

*E-mail: mark.nava@gmail.com.
*E-mail: parrinello@phys.chem.ethz.ch.

Notes

The authors declare no competing financial interest.

■ ACKNOWLEDGMENTS

All calculations were performed on the Brutus HPC cluster at ETH Zurich. We acknowledge the European Union Grant ERC-2009-AdG-247075, NCCR MARVEL [51NF40_141828], and the China Scholarship Council for funding.

■ REFERENCES

(1) Feynman, R. P.; Hibbs, A. R. *Quantum Mechanics and Path Integrals*; McGraw-Hill Companies: New York, 1965.
(2) Parrinello, M.; Rahman, A. *J. Chem. Phys.* **1984**, *80*, 860−867.
(3) Marx, D.; Parrinello, M. *J. Chem. Phys.* **1996**, *104*, 4077−4082.
(4) Nava, M.; Galli, D.; Cole, M. W.; Reatto, L. *Phys. Rev. B* **2012**, *86*, 174509.
(5) Stella, L.; Santoro, G. E.; Tosatti, E. *Phys. Rev. B* **2006**, *73*, 144302.
(6) Santoro, G. E.; Tosatti, E. *J. Phys. A: Math. Gen.* **2006**, *39*, R393.
(7) Brooke, J.; Bitko, D.; F, T.; Rosenbaum; Aeppli, G. *Science* **1999**, *284*, 779−781.
(8) Santoro, G. E.; Martonak, R.; Tosatti, E.; Car, R. *Science* **2002**, *295*, 2427−2430.
(9) Peng, Y.; Cao, Z.; Zhou, R.; Voth, G. *J. Chem. Theory Comput.* **2014**, *10*, 3634−3640.
(10) Wolynes, P. G.; Chandler, D. *J. Chem. Phys.* **1981**, *74*, 4078.
(11) Torrie, G.; Valleau, J. P. *J. Comput. Phys.* **1977**, *23*, 187.
(12) Wang, F.; Landau, D. P. *Phys. Rev. Lett.* **2001**, *86*, 2050.
(13) Darve, E.; Pohorille, A. *J. Chem. Phys.* **2001**, *115*, 9169.
(14) Laio, A.; Parrinello, M. *Proc. Natl. Acad. Sci.* **2002**, *99*, 12562.
(15) Barducci, A.; Bonomi, M.; Parrinello, M. *Comput. Mol. Sci.* **2011**, *1*, 826−843.
(16) Barducci, A.; Bussi, G.; Parrinello, M. *Phys. Rev. Lett.* **2008**, *100*, 020603.

DOI: 10.1021/ct501002a
J. Chem. Theory Comput. 2015, 11, 1383−1388

(17) Crespo, Y.; Laio, A.; Santoro, G.; Tosatti, E. *Phys. Rev. E* **2009**, *80*, 015702.
(18) Hall, R. W.; Berne, B. J. *J. Chem. Phys.* **1984**, *81*, 3641−3643.
(19) Ceriotti, M.; Bussi, G.; Parrinello, M. *Phys. Rev. Lett.* **2009**, *102*, 020601.
(20) Parrinello, M.; Rahman, A. *Phys. Rev. Lett.* **1980**, *45*, 1196−1199.
(21) Parrinello, M.; Rahman, A. J. *J. Appl. Phys.* **1981**, *52*, 7182−7190.
(22) Habershon, S.; Manolopoulos, D. E.; Markland, T. E.; Miller, T. F., III *Annu. Rev. Phys. Chem.* **2013**, *64*, 387−413.
(23) Bonomi, M.; Parrinello, M. *Phys. Rev. Lett.* **2010**, *104*, 190601.
(24) Dama, J. F.; Parrinello, M.; Voth, G. A. *Phys. Rev. Lett.* **2014**, *112*, 240602.
(25) Valsson, O.; Parrinello, M. *J. Chem. Theory. Comput.* **2013**, *9*, 5267.
(26) Tiwary, P.; Parrinello, M. *J. Phys. Chem. B* **2014**, *119*, 736−742 DOI: 10.1021/jp504920s.
(27) Liu, P.; Berne, B. J. *J. Chem. Phys.* **2003**, *118*, 2999−3005.
(28) Lee, Y. H.; Berne, B. J. *J. Phys. Chem. A* **2001**, *105*, 459−464.
(29) Gillan, M. J. *Philos. Mag. A* **1988**, *58*, 257−283.
(30) Gillan, M. J.; Christodoulos, F. *Int. J. Mod. Phys. C* **1993**, *04* (02), 287−297.
(31) Gillan, M. J. *J. Phys. C: Solid State Phys.* **1986**, *19*, 6169.
(32) Ceriotti, M.; Brain, G. A. R.; Riordan, O.; Manolopoulos, D. E. *Proc. R. Soc. A* **2012**, *468*, 2.
(33) Stella, L.; Santoro, G.; Tosatti, E. *Phys. Rev. B* **2006**, *73*, 144302.

DOI: 10.1021/ct501002a
J. Chem. Theory Comput. 2015, 11, 1383−1388